SEMARAK ILMU PUBLISHING

Journal of Advanced Research in Numerical Heat Transfer

Journal homepage:
https://semarakilmu.com.my/journals/index.php/arnht/index
ISSN: 2735-0142

Mixed Convection Boundary Layer Flow on A Vertical Flat Plate in Al_2O_3–Ag/Water Hybrid Nanofluid with Viscous Dissipation Effects

Eddy Elfiano[1,2], Nik Mohd Izual Nik Ibrahim[2,*], Muhammad Khairul Anuar Mohamed[3]

[1] Department of Mechanical Engineering, Faculty of Engineering Universitas Islam Riau, 28284 Pekanbaru, Provinsi Riau, Indonesia
[2] Faculty of Engineering and Technology DRB-HICOM University of Automotive Malaysia, Peramu Jaya Industrial Area, 26070 Pekan, Pahang, Malaysia
[3] Centre for Mathematical Sciences Universiti Malaysia Pahang, Lebuhraya Persiaran Tun Khalil Yaakob, 26300 Kuantan, Pahang, Malaysia

ARTICLE INFO

Article history:
Received 29 April 2024
Received in revised form 21 May 2024
Accepted 29 June 2024
Available online 30 July 2024

Keywords:
Mixed convection; Hybrid nanofluid; Vertical flat plate; Viscous dissipation

ABSTRACT

The present research examined the mixed convection boundary layer flow and heat transfer of hybrid nanofluid on a vertical flat plate with various volume concentrations and viscous dissipation effects. The governing non-linear partial differential equations are first transformed to a system of ordinary differential equations through the use of a similarity transformation. Subsequently, these equations are solved numerically using the Runge-Kutta-Fehlberg (RKF45) method in MAPLE. The numerical solution is computed for the temperature profiles, velocity profiles, reduced Nusselt number and reduced skin friction coefficient. The characteristics of flow and heat transfer for the Eckert number, the mixed convection parameter, and the hybrid nanoparticles volume fraction are analyzed and discussed. Numerical analysis demonstrates that increases in the λ value results in a decreasing in the thickness of the thermal boundary layer, Also, variations in the Ec values have no effect on the velocity profiles. The Ag-Al_2O_3/ water-based hybrid nanofluid examined in this study achieves comparable results to the Ag-water-based nanofluid.

1. Introduction

The flow of convective heat transfer on the surface of a vertical flat plate is a significant subject to investigate. Because of its contributions for engineering and commercial applications include fins of engine cylinder block, radiator fins, electronic components and turbine blades can also be modelled as flat plates with sufficient precision. The concept of convective heat transfer on flat plate was studied for the first time by Heinrich Blasius with his publication in 1908, where he derived the fluid profile for 2D boundary-layer flow over both a flat plate and circular cylinder [1]. While traditional heat transfer fluids like oil, water, and ethylene glycol mixes are inefficient at transferring heat. The use of nanofluids may enhance thermal conductivity by fluid flow, which is the coefficient of heat transfer between the heat transfer medium and the heat transfer surface [2]. Several

* *Corresponding author.*
E-mail address: izual@dhu.edu.my (Nik Mohd Izual Nik Ibrahim)

https://doi.org/10.37934/arnht.22.1.113

researchers have also conducted investigations on the flow of the boundary layer across a flat plate immersed in a nanofluid. Uddin *et al.,* [3] investigated that the volume fraction of nanoparticles is found to decrease as the linear momentum slip parameter increases, moreover that the nanoparticle volume fraction increases as the convective heat transfer parameter increases. Trimbitas *et al.,* [4] found that the range of the mixed convection parameter λ, within which the similarity solution is present, is greater in the event of an assisting flow compared to the opposing flow case. Sahu *et al.,* [5] presented that the velocity of both buoyancy-induced assisting and opposing flows increases as the volume fraction of Cu nanoparticles increases, however, the rate of increase is slowed when there is an opposing flow. Astuti *et al.,* [6] studied three distinct categories of water-based nanofluids, specifically those containing copper Cu, Aluminum oxide Al_2O_3, and Titanium dioxide TiO_2. Observations indicate that the velocity profiles of TiO_2-water and Al_2O_3-water exhibit similarities due to the near proximity of their densities and thermal expansion coefficients.

The economic challenges related to the application of nanofluids have led researchers to investigate materials that possess the potential to address these limitations. Hybrid nanofluids represent a novel category of nanofluids for heat transfer applications, wherein two distinct types of nanoparticles are dispersed within heat transfer fluid. However, there is limited of research conducted on boundary layer flows utilizing hybrid nanofluids. Based on the available information, there are several research papers by Dinarvand and Nademi [7] studied mixed convection $Cu-Ag/water$ hybrid nanofluid a long vertical cylinder. Rosca *et al*., [8] studied on the mixed convection stagnation point of classical viscous fluids past a vertical plate flow. Meanwhile, Zainal *et al*., [9] presented investigates the phenomenon of unsteady mixed convection in a flow of Al_2O_3-Cu/H_2O hybrid nanofluid at the stagnation point, as it passes a vertical plate. Doley *et al.,* [10] and Khan *et al*., [11] focused in free convective flow of a hybrid nanofluid across a vertical plate.

In recent research investigations, the phenomenon of fluid flow on a vertical flat plate within a hybrid nanofluid has been examined. These studies involve a range of research activities, including the previous publications. Yaseen *et al*., [12] explored the MHD nonlinear convective SiO_2/water nanofluid and SiO_2–MoS_2/water hybrid nanofluid flow and heat transport over a vertical flat plate. The study revealed that the velocity profile of the SiO_2–MoS_2/water hybrid nanofluid shows a higher magnitude compared to that of the SiO_2/water nanofluid. Furthermore, the increase in the volume fraction of nanoparticles leads to a corresponding increase in the velocity of both hybrid nanofluid and nanofluid. Wahid *et al*., [13] investigated the mixed convection flow of a hybrid nanofluid past a permeable vertical flat plate with thermal radiation effect. It is discovered that by decreasing the concentration volume of copper and raising the magnetic and radiation parameters, the separation of the boundary layer can be impeded. Lastly, a compelling investigation conducted by Wahid *et al*., [14] studied hybrid nanofluid radiative mixed convection stagnation point flow past a vertical flat plate.

It is noteworthy to emphasize that the investigation of convective heat transfer on a vertical flat plate remains a subject of ongoing research. Hence, the objective of the current work is to examine the mixed convection boundary layer flow over on a vertical flat plate in Al_2O_3–Ag/water hybrid nanofluid with viscous dissipation effects. The governing Partial Differential Equations (PDEs) are solved using numerical methods, and the modification of relevant physical properties has not been previously explored. Therefore, the results presented in this investigation are original.

2. Mathematical Formulations

A constant two-dimensional boundary layer flow across a vertical flat plate immersed in an ambient temperature hybrid nanofluid is assumed, T_∞ as illustrated in Figure 1. Let T denote the temperature within the boundary layer, T_w is the temperature of the wall. u_∞ is the free stream velocity and $u_w(x) = \varepsilon u_\infty$ is the fluid velocity where ε is the fluid velocity parameter. The boundary layer equations that can be produced are as follows [15,16]:

$$\frac{\partial u}{\partial x} + \frac{\partial v}{\partial y} = 0 \tag{1}$$

$$u\,\frac{\partial u}{\partial x} + v\frac{\partial u}{\partial y} = \frac{\mu_{hnf}}{\rho_{hnf}}\frac{\partial^2 u}{\partial y^2} + \frac{(\rho\beta)_{hnf}}{\rho_{hnf}}\,g(T - T_\infty) \tag{2}$$

$$u\frac{\partial T}{\partial x} + v\frac{\partial T}{\partial y} = \frac{k_{hnf}}{(\rho C_p)_{hnf}}\frac{\partial^2 T}{\partial y^2} + \frac{\mu_{hnf}}{(\rho C_p)_{hnf}}\left(\frac{\partial u}{\partial y}\right)^2 \tag{3}$$

subjected to the boundary condition:

$$\begin{aligned} &u = u_w(x) = \varepsilon u_\infty, \quad v = 0,\ T = T_w \quad \text{at} \quad y = 0 \\ &u = u_\infty,\ T \to T_w \quad \text{as} \quad y \to \infty \end{aligned} \tag{4}$$

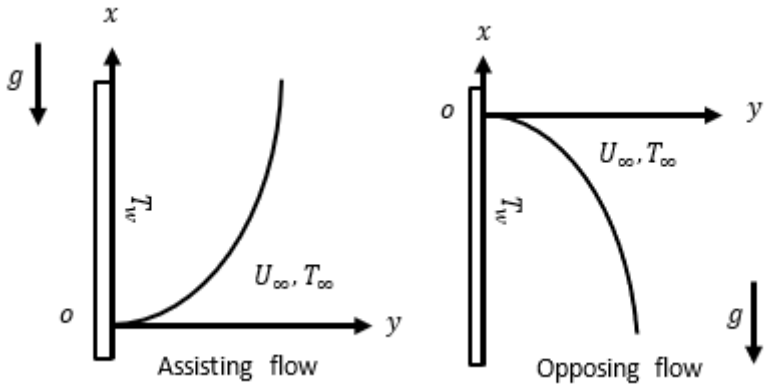

Fig. 1. Physical model and the coordinate system [16]

where u and v are the velocity components along the x and y axes, respectively. μ_{hnf} is the dynamic viscosity of hybrid nanofluid, ρ_{hnf} is the hybrid nanofluid density, g is the gravity acceleration, β_{hnf} is the hybrid nanofluid thermal expansion, $(\rho C_p)_{hnf}$ is the heat capacity of hybrid nanofluid, v_{hnf} is the kinematic viscosity of hybrid nanofluid and lastly, k_{hnf} is the thermal conductivity of hybrid nanofluid which can be expressed as follows [17,18]:

$$v_{hnf} = \frac{\mu_{hnf}}{\rho_{hnf}},\ \mu_{hnf} = \frac{\mu_f}{(1-\phi_1)^{2.5}(1-\phi_2)^{2.5}}, \rho_{hnf} = (1-\phi_2)\left[(1-\phi_1)\rho_f + \phi_1\rho_{s1}\right] + \phi_2\rho_{s2},$$
$$(\rho\beta)_{hnf} = (1-\phi_2)\left[(1-\phi_1)(\rho\beta)_f + \phi_1(\rho\beta)_{s1}\right] + \phi_2(\rho\beta)_{s2}$$
$$\left(\rho C_p\right)_{hnf} = (1-\phi_2)\left[(1-\phi_1)\left(\rho C_p\right)_f + \phi_1\left(\rho C_p\right)_{s1}\right] + \phi_2\left(\rho C_p\right)_{s2},$$
$$\frac{k_{hnf}}{k_{bf}} = \frac{k_{s2} + 2k_{bf} - 2\phi_2\left(k_{bf} - k_{s2}\right)}{k_{s2} + 2k_{bf} + \phi_2\left(k_{bf} - k_{s2}\right)}, \qquad \frac{k_{bf}}{k_f} = \frac{k_{s1} + 2k_f - 2\phi_1\left(k_f - k_{s1}\right)}{k_{s1} + 2k_f + \phi_1\left(k_f - k_{s1}\right)} \tag{5}$$

The subscript *hnf, f, s1* and *s2* represent the physical attributes of hybrid nanofluid, base fluid, alumina Al_2O_3 nanoparticle, and silver Ag nanoparticle, respectively. In the present study, a 0.06 vol. solid nanoparticle of Ag (ϕ_2= 0.06) is mixed with a water-based fluid to create Ag/water nanofluid. Meanwhile, 0.1 vol. solid nanoparticle of Al_2O_3 (ϕ_1= 0.1) is added with Ag/water nanofluid to form the Al_2O_3-Ag/water hybrid nanofluid.

The similarity transformation for E. (1)-(3) subjected to the boundary condition (4)

$$\eta = \left[\frac{u_\infty}{vx}\right]^{1/2} y, \qquad \psi = (u_\infty vx)^{1/2} f(\eta), \qquad \theta(\eta) = \frac{T-T_\infty}{T_w-T_\infty} \tag{6}$$

where η, θ and ψ are non-dimensional similarity variable, temperature and stream function. The Eq. (1) is satisfied by definition of $u = \frac{\partial\psi}{\partial y}$ and $v = -\frac{\partial\psi}{\partial x}$, respectively. Then, u and v can be derived as

$$u = u_\infty f'(\eta), \quad v = \frac{u_\infty y}{2x} f' - \left(\frac{u_\infty v}{x}\right)^{1/2} \frac{f}{2} \tag{7}$$

Next, the Eq. (5) and (6) are substitute into Eq. (2) and (3) which gives the following ordinary differential equations (ODEs) as follows:

$$\frac{v_{hnf}}{v_f} f''' + \frac{ff''}{2} + \frac{(\rho\beta)_{hnf}}{\rho_{hnf}\beta_f}\lambda\theta = 0 \tag{8}$$

$$\frac{1}{Pr}\ ac\ \theta'' + \frac{f\theta'}{2} + ad\ Ecf''^2 = 0 \tag{9}$$

Other dimensionless expressions, such as Gr, Re, Ec and λ, respectively represent for the Grashof, Reynold, Eckert and Richardson numbers.

$$Gr = \frac{g\beta_f(T_w-T_\infty)x\theta}{{u_\infty}^2}, \quad Re = \frac{u_\infty x}{v_f}, \ Ec = \frac{{U_\infty}^2}{Cp_f(T_w-T_\infty)}, \quad \lambda = \frac{Gr}{Re^2}$$

In order that the similarity solution for Eq. (8) and (9) exist, it is assumed [19,20]

$$\beta = mx^{-1} \tag{10}$$

where m is constant. Note that the assumption in Eq. (10) is necessary for the Eq. (8) and (9) to be independent of x. The boundary condition (4) become

$$f(0) = 0,\ f'(0) = \varepsilon, \qquad \theta(0) = 1$$
$$f'(\eta) \to 1,\ \theta(\eta) \to 0, \qquad as\ y \to \infty \tag{11}$$

The physical quantity interests are the wall temperature $\theta(0)$, the heat transfer rate $-\theta(0)$ and the skin friction coefficient C_f which given by

$$C_f = \frac{\tau_w}{\rho_f {u_\infty}^2} \tag{12}$$

with surface shear stress $\tau_w = \mu_{hnf}\left(\frac{\partial u}{\partial y}\right)_{y=0}$. Using the similarity variables in (6) gives

$$C_f (Re/2)^{1/2} = \frac{f''(0)}{(1-\varphi)^{2.5}} \tag{13}$$

which are referred as the reduce skin friction coefficient.

Other hybrid nanofluid quantities are listed below [21]:

1. $$\frac{v_{hnf}}{v_f} = \frac{1}{(1-\phi_1)^{2.5}(1-\phi_2)^{2.5}(1-\phi_2)\left[(1-\phi_1) + \phi_1\left(\rho_{s1}/\rho_f\right)\right] + \phi_2\left(\rho_{s2}/\rho_f\right)}$$

2. $$\frac{(\rho\beta)_{hnf}}{\rho_{hnf}\beta_f} = \frac{(1-\phi_2)\left[(1-\phi_1)\rho_f + \phi_1(\rho\beta)_{s1}/\beta_f\right] + \phi_2(\rho\beta)_{s2}/\beta_f}{(1-\phi_2)\left[(1-\phi_1)\rho_f + \phi_1\rho_{s1}\right] + \phi_2\rho_{s2}}$$

3. $$\frac{k_{hnf}\left(\rho C_p\right)_f}{k_f\left(\rho C_p\right)_{hnf}} = \frac{k_{hnf}/k_f}{(1-\phi_2)\left[(1-\phi_1) + \phi_1\left(\rho C_p\right)_{s1}/\left(\rho C_p\right)_f\right] + \phi_2\left(\rho C_p\right)_{s2}/\left(\rho C_p\right)_f}$$

4. $$\frac{\rho_{hnf}\left(C_p\right)_f}{\left(\rho C_p\right)_{hnf}} = \frac{(1-\phi_2)\left[(1-\phi_1)\rho_f + \phi_1\rho_{s1}\right] + \phi_2\rho_{s2}}{(1-\phi_2)\left[(1-\phi_1)\rho_f + \phi_1\left(\rho C_p\right)_{s1}/\left(C_p\right)_f\right] + \phi_2\left(\rho C_p\right)_{s2}/\left(C_p\right)_f}$$

3. Results and Discussions

The known Runge-Kutta-Fehlberg method is used to numerically solve the ordinary differential equations (8-9) subject to boundary conditions (11). This method, also known as RKF45, implements a 4th order approximation with an error estimator of order 5. The boundary layer thickness ranging from 7 to 10 is considered adequate for obtaining precise numerical results. Three relevant factors, namely the Prandtl number (Pr), the mixed convection parameter (λ), and the Eckert number (Ec) are taken into consideration. The nanoparticles Copper Cu, Silver Ag, Alumina oxide Al_2O_3, and Titanium oxide TiO_2 were tested with water as the base fluid. The thermophysical characteristics of nanoparticles are presented in Table 1. To evaluate the success of the numerical method and mathematical formulation employed, a comparative analysis have been performed with previously investigated results. Table 2 shows a comparison of the obtained results with the previously published findings for Al_2O_3 /water and TiO_2/water nanofluid, as reported by references [22-

24].The findings of this study demonstrate an excellent degree of agreement among the outcomes, which inspires trust in the accuracy and reliability of the overall findings.

Table 1
Water and nanoparticle thermophysical characteristics [24]

Physical Properties	Water (*f*)	Al_2O_3 (ϕ_1)	Ag (ϕ_1)	TiO_2 (ϕ_2)	*Cu*
ρ (kg/m^3)	997	3970	10500	4250	8933
Cp (J/kg.K)	4179	765	235	686.2	385
k (W/m.K)	0.613	40	429	8.95	400

Table 2
Value of $C_f Re_x^{1/2}$ in comparison to previously reported findings of various ϕ_1 for Al_2O_3 /Ag-water and $TiO_2/water$ when $Ec = \lambda = \phi_2 = 0$ and $Pr = 6.2$

ϕ_1	Al_2O_3 /$water$				$TiO_2/water$		
	Blasius [22]	Ahmad [23]	Mohamed [24]	Present	Blasius [22]	Ahmad [23]	Present
0	0.3321	0.3321	0.33205	0.332057	0.3321	0.3321	0.33205
0.002		0.3339	0.33388	0.333880		0.3340	0.33397
0.004		0.3357	0.33571	0.335709		0.3359	0.33589
0.008		0.3394	0.33939	0.339384		0.3398	0.33975
0.01		0.3412	0.34123	0.341231		0.3417	0.34169
0.02		0.3506	0.35056	0.350556		0.3515	0.35148
0.1		0.4316	0.43161	0.431591		0.4362	0.43623
0.2		0.5545	0.55451	0.554509		0.5642	0.56418

Graphs of results demonstrate the temperature profiles (θ) and velocity profiles for different values of parameter λ and the Eckert number (Ec), which represents the viscous dissipation parameter. Based on the temperature profiles shown in Figure 2, it can be observed that the addition of the viscous dissipation effect, leads to an enlargement in the thickness of the thermal boundary layer. An increase in the Eckert number leads to an augmentation in the kinetic energy and a corresponding amplification in the dissipation effects resulting from internal fluid friction. This phenomenon will lead to self-heating, thereby causing a change in the temperature gradient.

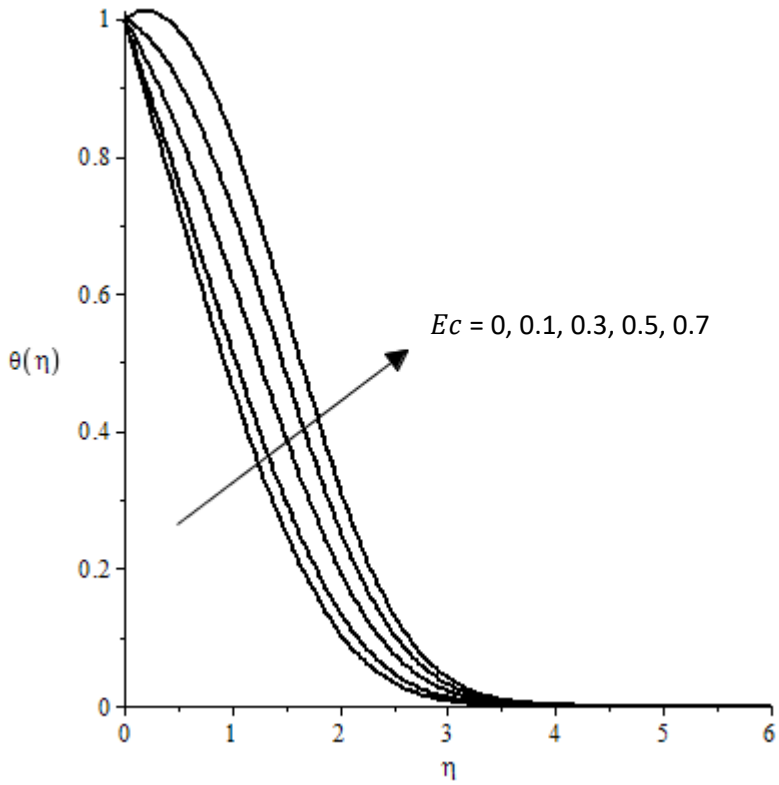

Fig. 2. Temperature profiles $\theta(\eta)$ for Ec when $Pr = 6.2$, $\phi_1 = 0.1$, $\phi_2 = 0.06$ and λ = 0

Based to the findings presented in Figure 3, it can be observed that an increase in the λ value leads to a decrease in thickness of the thermal boundary layer. This phenomenon is due to the dominance of buoyancy force over inertial force. From the numerical computation, the varies Ec values have no effect on the velocity profiles, as shown a unique curve in Figure 4. Physically, the viscous dissipation effect denoted by Ec is the transformation of kinetic energy into thermal energy, therefore, the velocity is constant. This provided evidence that viscous dissipation effects have no influence on the velocity boundary layer thickness, velocity gradient, or skin friction coefficient. In Figure 5, it can be observed that the increase of mixed convection parameter leads to an increase of the velocity boundary layer, whereas a negative mixed convection value has the opposite effect. The appearance of this problems can also be due to the large buoyancy force produced by the fluid.

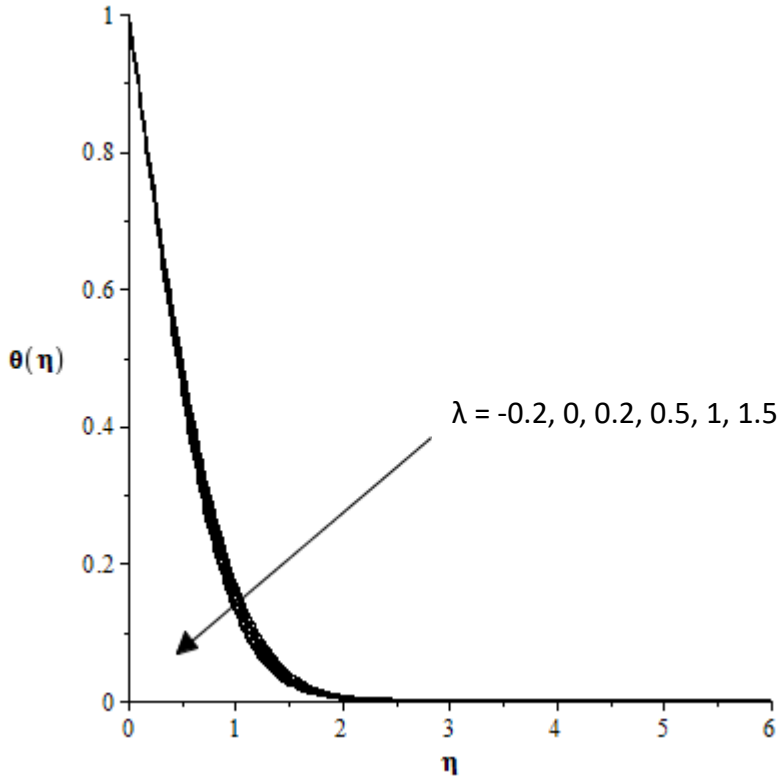

Fig. 3. Temperature profiles $\theta(\eta)$ for λ when $Ec = \phi_1 = 0.1$, $\phi_2 = 0.06$ and $Pr = 6.2$

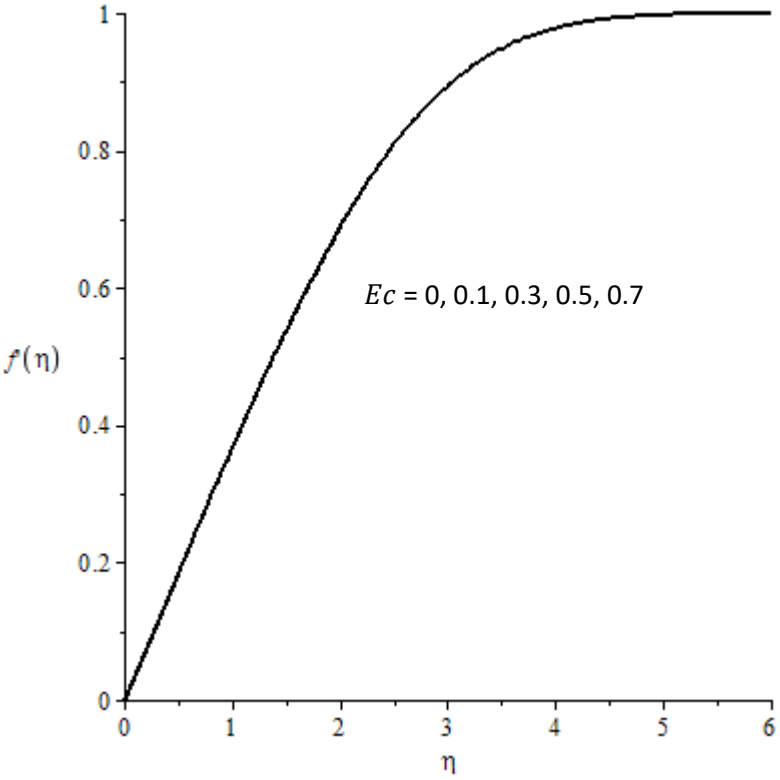

Fig. 4. Velocity profiles $f'(\eta)$ for Ec when $Pr = 6.2$, $\phi_1 = 0.1$, $\phi_2 = 0.06$ and $\lambda = 0$

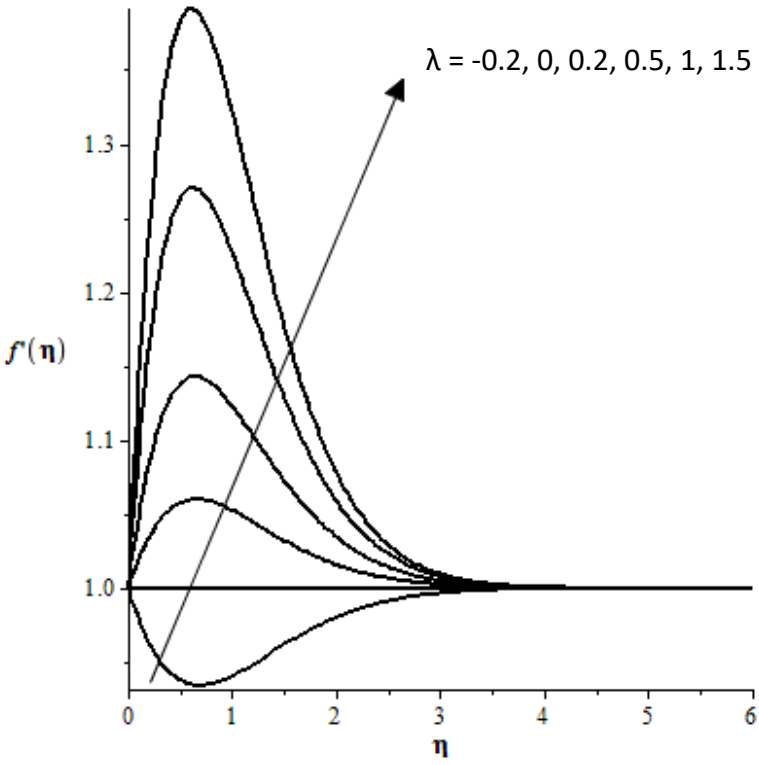

Fig. 5. Velocity profiles $f'(\eta)$ for λ when $Ec = \phi_1 = 0.1$, $\phi_2 = 0.06$ and $Pr = 6.2$

Figure 6 shows the distribution of velocity profiles with different values of epsilon, ε. The velocity ratio parameter is denoted by $\varepsilon = u_w/u_\sim$. $\varepsilon = 0$ (moving fluid or stationary plate), $\varepsilon = 1$ (velocity of fluid = velocity of plate) and $\varepsilon > 1$ (velocity of plate is faster than velocity of fluid). The assumption is made that the solid particle behaves like a fluid. Figure 6 illustrates that when $\varepsilon = 0$, the fluid velocity is significantly higher in comparison to cases where $\varepsilon = 1$ and $\varepsilon > 1$.

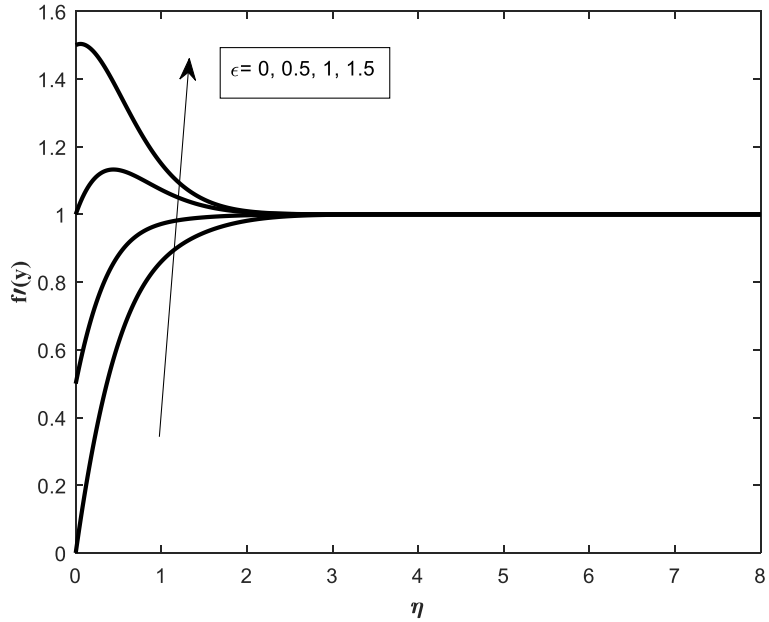

Fig. 6. Velocity profile $f'(y)$ for various value of ε when $Pr = 6.2$, $\lambda = 1$ and $Ec = \phi_1 = 0.1, \phi_2 = 0.06$

Figure 7 shows the distribution of reduced Nusselt number $Nu_x Re_x^{-1/2}$ with different values of Ec. This study examines four distinct forms of fluid, mainly those that are water-based ($\phi_1 = \phi_2 = 0$), 0.1 vol. Al_2O_3/water nanofluid ($\phi_1 = 0.1,\ \phi_2 = 0$), Ag-Al_2O_3/water hybrid nanofluid ($\phi_1 = 0.1,\ \phi_2 = 0.06$), and the 0.16 vol. Ag/water nanofluid. Particularly Ag Water/nanofluid mixture containing metal nanoparticles Ag with high-density and thermal conductivity. According to the data presented in Figure 7, the Ag /Water nanofluid exhibited the greatest $Nu_x Re_x^{-1/2}$ value, with the following closely Ag-Al_2O_3/water hybrid nanofluid. The fluid that is based on water exhibited the lowest score, indicating a very limited convective heat transfer performance when compared to other nanofluids. Formally, large values of Ec enhance heat transfer capability. The use of Ag Water, nanofluid is considered feasible due to the significantly higher thermal conductivity exhibited by Ag nanoparticles in comparison to other nanoparticles that have been examined. However, it is imperative to take consideration of the role of nano oxide in order to achieve cost reduction for mass production.

Finally, Figure 8 illustrates the distribution variation of $C_f Re_x^{1/2}$ for different values of λ. The analysis of the figure reveals that the introduction of a ($\lambda < 0$) value has resulted in a decrease in the skin values. The enhancement of the parameter λ results in an elevation of the skin friction coefficient. The Ag/water nanofluid exhibited the highest $C_f Re_x^{1/2}$ score, with the Ag-Al_2O_3/water hybrid nanofluid following closely behind. The increase of nanoparticle concentration within a fluid, associated with the higher density of these nanoparticles, have resulted in an escalation of the skin friction coefficient. The findings of this investigation indicate that the $C_f Re_x^{1/2}$ value remains constant with all concentrations of nano particles in relation to the Ec value.

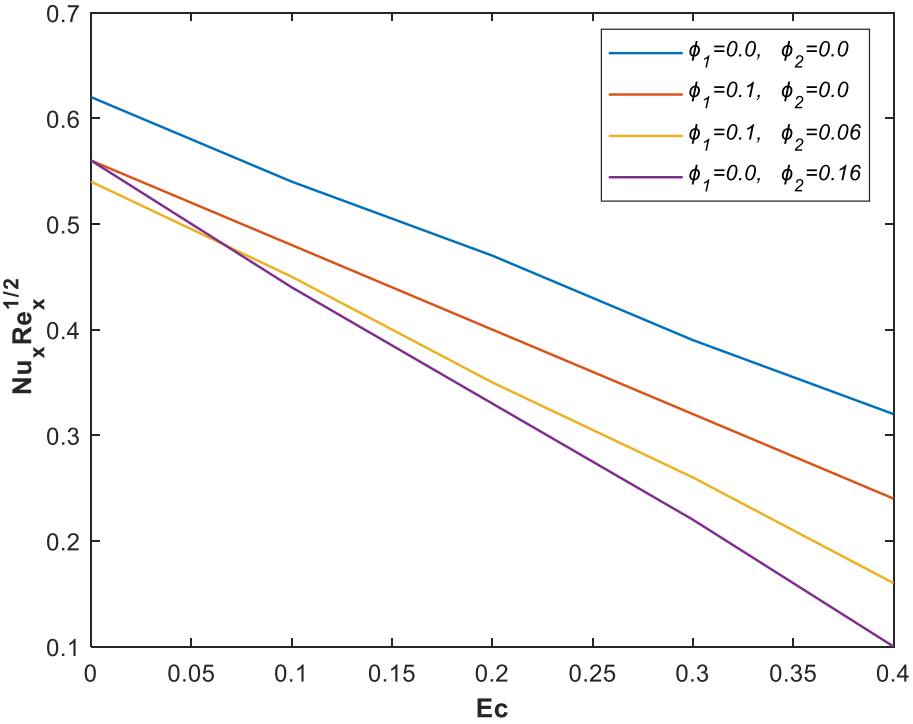

Fig. 7. Distribution of $Nu_x Re_x^{-1/2}$to Ec when $Pr = 6.2$ and $\lambda = 0$

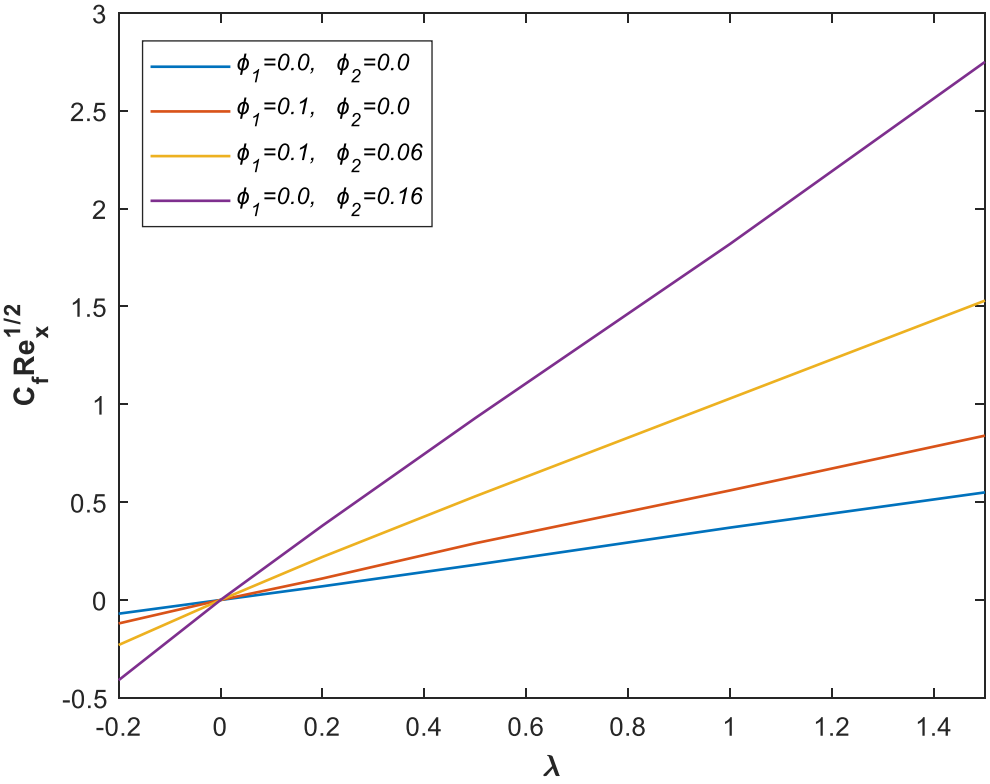

Fig. 8. Distribution of $C_f Re_x^{1/2}$ to λ when $Pr = 6.2$ and $Ec = 0$

4. Conclusions

As a conclusion, the enlargement of Ec value leads to greater temperature profiles $\theta(\eta)$ and thermal boundary layer thicknesses. In contrast, it can be noticed that an increase in the λ value results to a decrease in the thickness of the thermal boundary layer. This phenomenon occurs because buoyancy force predominates over inertial force. Based on the results obtained from numerical computation, it can be concluded that the different values of Ec lack any influence on the velocity profiles. The results of this study demonstrated that the thickness of the velocity boundary layer remains unchanged by the influence of viscous dissipation effects. In addition, the Ag-Al_2O_3/water hybrid nanofluid examined in this investigation demonstrates comparable outcomes to the Ag-water nanofluid. This indicates the possibility of hybrid nanofluids as an alternative to nanofluids, particularly in cases where costly nanomaterials are applied.

Acknowledgement

Authors gratefully acknowledge the financial and facilities support from the Malaysia Ministry of Education (FRGS/1/2019/STG06/ DHUAM/02/1), DRB-HICOM University of Automotive Malaysia.

References

[1] Jessee, Robert. An analytic solution of the thermal boundary layer at the leading edge of a heated semi-infinite flat plate under forced uniform flow. Louisiana State University and Agricultural & Mechanical College, 2015. https://digitalcommons.lsu.edu/gradschool_theses.

[2] ThAM, LEONy, and ROSLiNdA NAzAR. "Mixed convection flow about a solid sphere embedded in a porous medium filled with a nanofluid." (2012): 1643-1649. http://oai:generic.eprints.org:5684/core365.

[3] Uddin, Jashim, and I. Pop. "Free convection boundary layer flow of a nanofluid from a convectively heated vertical plate with linear momentum slip boundary condition." Sains Malaysiana 41 (2012): 1475-1482. http://journalarticle.ukm.my/5585/.

[4] Trîmbiţaş, R., T. Grosan, and I. Pop. "Mixed convection boundary layer flow past vertical flat plate in nanofluid: case of prescribed wall heat flux." Applied Mathematics and Mechanics 36, no. 8 (2015): 1091-1104. http://doi.org/10.1007/s10483-015-1967-7.

[5] Sahu, A. K., Maji, S and Yadav, K.. Local similarity solution of mixed convection boundary layer flow over a vertical flat plate for nanofluids. International journal of innovative research in science and engineering, 2016. http://www.ijirse.com/wp-content/upload/2016/02/220ijirse.pdf

[6] Kaprawi, S., H. Astuti, and P. Sri. "Natural convection of nanofluids past an accelerated vertical plate with variable wall temperature by presence of the radiation." Frontiers in Heat and Mass Transfer (FHMT) 13 (2019). http://doi.org/10.5098/hmt.13.3

[7] Dinarvand, S. A. E. E. D., and M. Nademi Rostami. "Mixed convection of a Cu-Ag/water hybrid nanofluid along a vertical porous cylinder via modified Tiwari-Das model." J. Theor. Appl. Mech 49 (2019): 149-169. http://doi.org/10.7546/JTAM.49.19.02.05

[8] Roşca, Alin V., Natalia C. Roşca, and Ioan Pop. "Mixed convection stagnation point flow of a hybrid nanofluid past a vertical flat plate with a second order velocity model." International Journal of Numerical Methods for Heat & Fluid Flow 31, no. 1 (2021): 75-91. https://doi.org/10.1108/HFF-03-2020-0152

[9] Zainal, N. A., R. Nazar, K. Naganthran, and I. Pop. "Slip effects on unsteady mixed convection of hybrid nanofluid flow near the stagnation point." Applied Mathematics and Mechanics 43, no. 4 (2022): 547-556. https://doi.org/10.1007/s10483-022-2823-6

[10] Doley, Swapnali, A. Vanav Kumar, and Jino Lawrence. "Time fractional transient magnetohydrodynamic natural convection of hybrid nanofluid flow over an impulsively started vertical plate." Computational Thermal Sciences: An International Journal 14, no. 3 (2022). https://doi.org/10.1615/ComputThermalScien.2022041607

[11] Khan, Umair, Aurang Zaib, Sakhinah Abu Bakar, Nepal Chandra Roy, and Anuar Ishak. "Buoyancy effect on the stagnation point flow of a hybrid nanofluid toward a vertical plate in a saturated porous medium." Case Studies in Thermal Engineering 27 (2021): 101342. https://doi.org/10.1016/j.csite.2021.101342

[12] Yaseen, Moh, Rashmi Garia, Sawan Kumar Rawat, and Manoj Kumar. "Hybrid nanofluid flow over a vertical flat plate with Marangoni convection in the presence of quadratic thermal radiation and exponential heat source." International Journal of Ambient Energy 44, no. 1 (2023): 527-541. https://doi.org/10.1080/01430750.2022.2132287.

[13] Wahid, Nur Syahirah, Norihan Md Arifin, Najiyah Safwa Khashi'ie, Ioan Pop, Norfifah Bachok, and Mohd Ezad Hafidz Hafidzuddin. "MHD mixed convection flow of a hybrid nanofluid past a permeable vertical flat plate with thermal radiation effect." Alexandria Engineering Journal 61, no. 4 (2022): 3323-3333. https://doi.org/10.1016/j.aej.2021.08.059

[14] Wahid, Nur Syahirah, Norihan Md Arifin, Najiyah Safwa Khashi'ie, Ioan Pop, Norfifah Bachok, and Mohd Ezad Hafidz Hafidzuddin. "Hybrid nanofluid radiative mixed convection stagnation point flow past a vertical flat plate with Dufour and Soret effects." Mathematics 10, no. 16 (2022): 2966. https://doi.org/10.3390/math10162966

[15] Mohamed, Muhammad Khairul Anuar, Huei Ruey Ong, Mohd Zuki Salleh, and Basuki Widodo. "Mixed convection boundary layer flow of engine oil nanofluid on a vertical flat plate with viscous dissipation." Asean Journal of Automotive Technology 1, no. 1 (2019): 29-38. https://journal.dhuautomotive.edu.my/autojournal/article/view/7.

[16] Mohamed, Muhammad Khairul Anuar, Mohd Zuki Salleh, and Anuar Ishak. "Effects of viscous dissipation on mixed convection boundary layer flow past a vertical moving plate in a nanofluid." Journal of Advanced Research in Fluid Mechanics and Thermal Sciences 69, no. 2 (2020): 1-18. http://www.doi.org/10.37934/arfmts.69.2.118.

[17] Devi, Suriya Uma, and SP Anjali Devi. "Heat transfer enhancement of cu− $ al_ {2} o_ {3} $/water hybrid nanofluid flow over a stretching sheet." Journal of the Nigerian Mathematical Society 36, no. 2 (2017): 419-433. https://ojs.ictp.it/jnms/index.php/jnms/article/view/147.

[18] Mohamed, Muhammad Khairul Anuar, Huei Ruey Ong, Hamzah Taha Alkasasbeh, and Mohd Zuki Salleh. "Heat transfer of ag-Al2O3/water hybrid nanofluid on a stagnation point flow over a stretching sheet with newtonian heating." In Journal of Physics: Conference Series, vol. 1529, no. 4, p. 042085. IOP Publishing, 2020. https://doi:10.1088/1742-6596/1529/4/042085.

[19] Makinde, Oluwole D., and P. Oladapo Olanrewaju. "Buoyancy effects on thermal boundary layer over a vertical plate with a convective surface boundary condition." (2010): 044502. https://doi.org/10.1115/1.4001386.

[20] Ishak, Anuar. "Similarity solutions for flow and heat transfer over a permeable surface with convective boundary condition." Applied Mathematics and Computation 217, no. 2 (2010): 837-842. https://doi.org/10.1016/j.amc.2010.06.026.

[21] Mohamed, Muhammad Khairul Anuar, Mohd Zuki Salleh, Fadhilah Che Jamil, and Ong Huei. "Free convection boundary layer flow over a horizontal circular cylinder in Al2O3-Ag/water hybrid nanofluid with viscous dissipation." Malaysian Journal of Fundamental and Applied Sciences 17, no. 1 (2021): 20-25. https://doi.org/10.11113/mjfas.v17n1.1964.

[22] BLASIUS, H. "Grenzschichten in Flussigkeiten mit kleiner Reibung." Z. Math. Phys. 56 (1908): 1-37.
[23] Ahmad, Syakila, Azizah Mohd Rohni, and Ioan Pop. "Blasius and Sakiadis problems in nanofluids." Acta Mechanica 218 (2011): 195-204. https://doi.org/10.1007/s00707-010-0414-6
[24] MOHAMED, MUHAMMAD KHAIRUL ANUAR, A. Hussanan, H. T. Alkasasbeh, B. Widodo, and M. Z. Salleh. "Boundary layer flow on permeable flat surface in Ag-Al2O3/water hybrid nanofluid with viscous dissipation." Data Analytics and Applied Mathematics (DAAM) 2, no. 1 (2021): 11-19. https://doi.org/10.15282/daam.v2i1.6431